



Please cite the Published Version

Kim, Hobeom , Lim, Jaekeun, Sohail, Muhammad  and Nazeeruddin, Mohammad Khaja (2022) Superhalogen Passivation for Efficient and Stable Perovskite Solar Cells. Solar RRL, 6 (7). 2200013 ISSN 2367-198X

DOI: <https://doi.org/10.1002/solr.202200013>

Publisher: Wiley

Version: Published Version

Downloaded from: <https://e-space.mmu.ac.uk/635402/>

Usage rights:  [Creative Commons: Attribution 4.0](https://creativecommons.org/licenses/by/4.0/)

Additional Information: This is an open access article which first appeared in Solar RRL

Enquiries:

If you have questions about this document, contact openresearch@mmu.ac.uk. Please include the URL of the record in e-space. If you believe that your, or a third party's rights have been compromised through this document please see our Take Down policy (available from <https://www.mmu.ac.uk/library/using-the-library/policies-and-guidelines>)

Superhalogen Passivation for Efficient and Stable Perovskite Solar Cells

Hobeom Kim,* Jaekeun Lim, Muhammad Sohail,
and Mohammad Khaja Nazeeruddin*

Metal-halide perovskites are optoelectronic materials applied to solar cells as a light absorber due to their excellent optoelectronic properties. The power conversion efficiency of perovskite solar cells (PSCs) reaches 25.7% certified, which stands in comparison with Si solar cells. Importantly, compositional engineering of perovskites has been one of the keys to the breakthrough. However, the presence of defects within perovskites is a matter of importance as it can cause nonradiative recombination of charge carriers. In addition, defect migration can degrade the photovoltaic performance and stability of PSCs. Previous studies have commonly addressed that iodide-related defects such as interstitial iodide and iodide vacancy are problematic due to their low formation energy. Thus, halide engineering is imperative to mitigate the defect-related dynamics and improve the materials quality of perovskites. In this sense, superhalogen is a promising candidate for defect passivation and stabilization of perovskites based on its higher electronegativity and electron affinity than halides, which are beneficial to the formation of a more robust interaction with adjacent elements in perovskites. This perspective gives an overview of studies regarding the use of superhalogen to develop efficient and stable PSCs and concludes with an outlook of further research directions.

demonstrated a certified power conversion efficiency (PCE) of 25.7% being comparable to the existing photovoltaic technology of Si solar cells.^[2] The achievement of the high-efficiency PSCs can be attributed to the excellent optoelectronic properties of perovskite light absorbers with a high-absorption coefficient and long-range carrier diffusion length. Also, its simple fabrication process using low-cost materials opens a bright prospect of commercialization of PSCs in the energy industry. In general, the lattice structure of metal-halide perovskites consists of three distinct positions that formulate ABX₃ cubic unit cells, where cation A (e.g., methylammonium (MA⁺), formamidinium (FA⁺), and/or Cs⁺) is located at (0,0,0), cation B (e.g., Pb²⁺) is at (1/2,1/2,1/2), and halide X (e.g., Cl⁻, Br⁻, and I⁻) is at the center of the six planes of the cubic at (1/2,1/2,0) (Figure 1a).^[3] Therefore, when the Goldschmidt tolerance factor is between 0.8 and 1.0, and the octahedral factor is between 0.442 and 0.895, 3D perovskites

1. Introduction


Metal-halide perovskites are a class of optoelectronic materials for solar cells. Since Miyasaka et al. first reported perovskite solar cells (PSCs) based on a liquid junction in 2009,^[1] recent solid-state PSCs using 3D polycrystalline perovskites have

can be formulated with a high degree of freedom in terms of compositional engineering, which has enabled and will enable the advancement of perovskites as a light absorber.^[3,4]

Nevertheless, perovskites fundamentally suffer from their internal defects in the bulk and at the surface of their polycrystalline film.^[5–8] The presence of some defects accompanies the formation of electronic states within the bandgap of perovskites, leading to nonradiative recombination of excitons and charge carriers, thereby degrading photovoltaic characteristics of PSCs. Furthermore, the defects cause structural degradation of perovskites as they migrate due to their ionic nature.^[9] Certainly, deep-level defects are undesirable because they are primary nonradiative recombination center trapping excitons and charge carriers. In contrast, the so-called defect tolerance of perovskites, i.e., those with the benign nature of the shallow defects, has been known to enable efficient radiative recombination of charge carriers.^[10] However, the shallow-level defects may also be problematic as they can lead to the formation of polarons that may activate the nonradiative process degrading the photovoltaic performance of PSCs.^[11] Several studies have revealed that interstitial iodide and iodide vacancy are responsible for the formation of deep-, and shallow-level trap states, respectively,^[12,13] and their high density in perovskites due to the low formation energy may result

H. Kim, J. Lim, M. K. Nazeeruddin
Group for Molecular Engineering of Functional Materials
Institute of Chemical Sciences and Engineering
École Polytechnique Fédérale de Lausanne
CH-1951 Sion, Switzerland
E-mail: hobeom.kim@epfl.ch; mdkhaja.nazeeruddin@epfl.ch

M. Sohail
Science Department
Texas A&M University at Qatar
Education City, Doha 23874, Qatar

 The ORCID identification number(s) for the author(s) of this article can be found under <https://doi.org/10.1002/solr.202200013>.

© 2022 The Authors. Solar RRL published by Wiley-VCH GmbH. This is an open access article under the terms of the Creative Commons Attribution License, which permits use, distribution and reproduction in any medium, provided the original work is properly cited.

DOI: 10.1002/solr.202200013

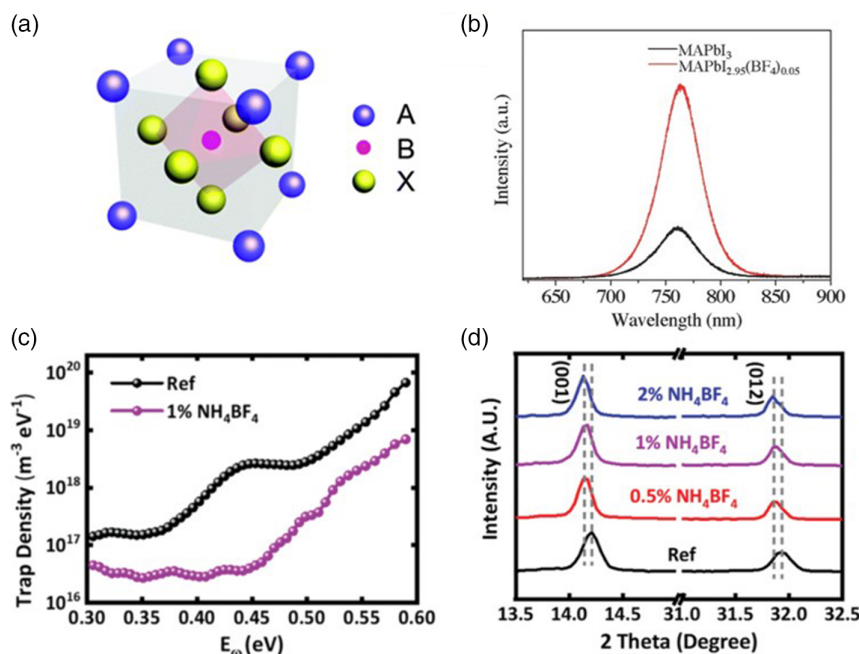


Figure 1. a) Crystal structure of metal-halide perovskite. Reproduced with permission.^[3] Copyright 2016, The Royal Society of Chemistry. b) Improvement in PL intensity by incorporating superhalogen (BF₄⁻) into perovskite (MAPbI₃). Reproduced with permission.^[23] Copyright 2015, Wiley-VCH. c) Reduction of trap density of states in the device using superhalogen-incorporated perovskite. d) XRD patterns of perovskites shifting to lower 2θ. Reproduced with permission.^[25] Copyright 2019, Wiley-VCH.

in more serious degradation of the material's optoelectronic properties and stability. Moreover, the most active migrating species is known to be iodide with a low activation energy of migration.^[14] Therefore, defect engineering, particularly the halide-related defects, maybe the key to further improvement in the efficiency and stability of PSCs.

In this sense, one of the most direct and effective approaches to mitigate the defect-related dynamics in perovskites may be to engineer the anion site by exploiting pseudo-halides with a valency of -1, which may fit into the X site of the perovskite lattice. For example, recently, Kim et al. reported the incorporation of a small amount of polyatomic pseudo-halide, HCOO⁻ into perovskites thereby demonstrating PSCs with a PCE of 25.6% and long-term operational stability.^[15] The authors presented the role of HCOO⁻ in the passivation of iodide vacancy, which is a predominant defect in iodide-based perovskites as above-mentioned. Also, thiocyanate (SCN⁻) has been the most widely used pseudo-halide to stabilize perovskites by occupying the X site in the perovskite lattice.^[16,17]

In fact, in the group of pseudo-halides, there is a specific class of molecules called superhalogen that is highly electronegative with a greater electron affinity than monoatomic halogens.^[18,19] Thus, strong interaction with adjacent cations in perovskites can be expected to suppress the formation of halide-related defects and stabilize perovskites. In this perspective, we present studies on the use of superhalogen molecules such as tetrafluoroborate (BF₄⁻), borohydride (BH₄⁻), and hexafluorophosphate (PF₆⁻) for defect passivation and enhancement of the structural stability of perovskites, which can lead to efficient radiative recombination and better device performance. As defect passivation of

perovskites is generally realized according to its target position, for example, either in the bulk or at the surface of a polycrystalline perovskite film, we accordingly organized sections separately dealing with the use of superhalogen in the bulk and for the surface treatment of perovskites. Lastly, we present an outlook on the use of superhalogen in perovskites with some suggestions for further advancements of PSCs.

2. Incorporation of Superhalogen in the Bulk of Perovskites

In 2014, Ogale et al. first introduced the use of superhalogen BF₄⁻ to incorporate it into methylammonium lead triiodide (MAPbI₃) with an idea of improving the photocurrent of perovskites inspired by a previous study in which fluorine-doped perovskites increased photocurrent of solid-state dye-sensitized solar cells.^[20,21] The formulation of perovskites incorporating superhalogen (MAPbI_(3-x)(BF₄)_x) was completed by a two-step deposition method, where PbI₂ was first deposited and subsequently exposed to MABF₄. Photodetectors using the perovskites exhibited an increased photo-response compared to control devices using pristine MAPbI₃. This study showed the potential of superhalogen in its application to PSCs. Walsh et al. (2014) reported exploration of the use of superhalogens, BF₄⁻ and PF₆⁻ in the framework of CsPbI₃ through computational studies showing possible partial substitution of superhalogen for iodide of perovskites.^[22] The first PSCs using superhalogen-incorporated perovskites, MAPbI_(3-x)(BF₄)_x, was demonstrated by Han et al. in 2015.^[23] The authors used a fully printable

hole-transporting material (HTM) free mesoscopic structure (FTO/(TiO₂/ZrO₂/carbon)/perovskite), in which perovskite is infiltrated into the underlying mesoporous TiO₂ and ZrO₂ scaffolds through the top mesoporous carbon electrode. The superhalogen-incorporated perovskites were obtained from a MAPbI₃ precursor solution with the addition of MABF₄. The perovskite film with BF₄⁻ exhibited improved photoluminescence (PL) intensity, which the authors attributed to fewer traps in the film compared to pristine MAPbI₃. (Figure 1b) Furthermore, electrochemical impedance spectroscopy (EIS) revealed that the incorporation of BF₄⁻ suppressed interfacial charge recombination and bulk recombination in the device, resulting in a PCE of 13.24%, which was higher than the otherwise-identical device using pristine MAPbI₃ (10.54%). Similarly, Hu et al. (2018) employed MABF₄ as an additive in a perovskite precursor solution consisting of MAPbI₃ and 5-ammonium valeric acid iodide (5-AVAI).^[24] The superhalogen-incorporated perovskites, (5-AVA)_{0.034}MA_{0.966}PbI_{3-x}(BF₄)_x showed an improvement in PL characteristics, which the authors also attributed to a decrease in defect density within the perovskite films as well as efficient electron extraction from the perovskite to underlying TiO₂. Thus, the HTM-free mesoscopic PSCs resulted in a PCE of 15.5%, which was higher than the control device without superhalogen (13.4%). In 2019, Jen et al. employed NH₄BF₄ to develop superhalogen-incorporated perovskites, FA_{0.83}MA_{0.17}Pb(I_{Br})_{3-x}(BF₄)_x.^[25] The incorporation of BF₄⁻ effectively reduced trap density in perovskites, which suppressed non-radiative recombination and improved PL characteristics (Figure 1c). PSCs using the perovskites in an n-i-p structure (ITO/SnO₂/perovskite/spiro-OMeTAD/MoO₃/Ag) achieved a PCE of 20.16%, which was higher than the device using perovskites without superhalogen (17.55%). The authors suggested that the improvements might be due to lattice expansion (and relaxation) of perovskites derived by the incorporation of BF₄⁻ based on a shift of (100) diffraction peak of the perovskite to a lower 2θ (Figure 1d). Given the similar ionic radius between I⁻ (220 pm) and BF₄⁻ (218 pm), the authors surmised that the lattice expansion might originate from a weaker bonding between BF₄⁻ and Pb²⁺ due to weaker hybridizations of tetrahedral BF₄⁻ with the atomic orbitals of Pb²⁺ than spherical I⁻.

The studies presented in the paragraph above commonly used a superhalogen compound containing MA⁺ in its cationic part that is already a constituent of perovskite, or NH₄⁺ that may not exert an additional function, but maybe evaporated during the formation of perovskite crystal. In contrast, some studies intended to take advantage of the cationic part of the superhalogen compound for a synergistic effect. Snaith et al. (2019) highlighted that the incorporation of ionic liquid (IL), 1-butyl-3-methylimidazolium tetrafluoroborate (BMIMBF₄) into perovskite ((FA_{0.83}MA_{0.17})_{0.95}CS_{0.05}Pb(I_{0.9}Br_{0.1})₃) improved the stability of the perovskite film and device as well as its efficiency.^[26] The authors assumed that BMIM⁺ bound at the surface and grain boundaries of the polycrystalline perovskite film based on its depth profile obtained by time-of-flight secondary ion mass spectrometry (ToF-SIMS) (Figure 2a). Therefore, the perovskite film was rendered highly resistant to external degradation factors such as oxygen and moisture (Figure 2b). Interestingly, the authors visualized ion migration in perovskites of a planar device (Au/perovskite/Au with a channel width of 150 μm) by PL imaging under a constant bias (Figure 2c). The control film without the ionic liquid (IL) showed PL quenching, which was attributed

to the accumulation of defects and/or the structural degradation of perovskites. We presume iodide was the migrating species considering the moving position of PL emission across the channel. In contrast, the IL incorporation prevented the PL quenching, which indicates effective suppression of ion migration in the perovskite film. Although the authors did not deal with the detail of the underlying reasons for the suppression of ion migration, we conjecture that the presence of BF₄⁻ at the grain boundary might contribute to the suppression of the ion migration because of the high binding affinity of BF₄⁻ to iodide vacancy (V_I⁺).^[27] The same research group (2020) reported the use of a different ionic compound, 1-butyl-1-methylpiperidinium tetrafluoroborate ([BMP]⁺[BF₄]⁻) to stabilize perovskites (Cs_{0.17}FA_{0.83}Pb(I_{1-x}Br_x)₃).^[28] The authors addressed the detrimentality of the formation of iodine (I₂) under illumination on the device stability,^[29] and explained that it forms due to the formation of Frenkel defects consisting of iodide vacancies and/or their interstitial pairs. The authors postulated that the IL compound could passivate sites available for the iodide oxidation, and suppress the migration of halide species. Oh et al. (2020) proposed to use ionic imidazolium tetrafluoroborate (IMBF₄) in mixed Pb-Sn perovskites.^[30] The mixed Pb-Sn perovskites, due to the different ionic radii between Sn (1.18 Å) and Pb (1.19 Å), are vulnerable to lattice strain by lattice distortion that can lead to defect formation. The authors conjectured that the incorporation of a smaller BF₄⁻ than I⁻ could relieve the strain by releasing strong tension between Pb and I. However, the X-ray diffraction (XRD) showed a shift implying the lattice expansion, and the authors ascribed it to the less strong hybridization of BF₄⁻ with the Pb atomic orbitals compared to I⁻ as proposed by Jen et al. previously. As the lattice relaxation increases the formation energy of V_I, the incorporation of BF₄⁻ into the perovskite lattice is expected to result in less density of V_I suppressing iodide oxidation. Concomitantly, the undesirable reduction of metallic species that yield Pb⁰ and Sn⁰ can be inhibited. In contrast, the cationic part (IM⁺) of the ionic compound may passivate positively charged under-coordinated Pb²⁺ or Sn²⁺. Based on the synergistic effect of IMBF₄, the best-performing device showed PCEs over 19.0% with improved stability while the otherwise-identical device without the superhalogen compound achieved lower PCEs ≈17% with a shorter device lifetime. Song et al. (2021) reported the use of zwitterionic ionic liquid (ZIL) that contains 4-fluoro-phenyl ammonium (4FB⁺) as a cation and tetrafluoroborate (BF₄⁻) as an anion in a two-step solution-processed (FAPbI₃)_{1-x}(MAPbBr₃)_x.^[31] The authors suggested that 4FB⁺ and BF₄⁻ can effectively passivate defects in perovskites by filling corresponding vacancies, which are formed by migration of the A-site cation and the X-site halide, respectively (Figure 2d). Furthermore, the passivation of under-coordinated Pb²⁺ by 4FB⁺ was suggested owing to its electron-donating property. Accordingly, the reduction of trap state density was empirically shown. However, the XRD peak of (001) of the perovskite exhibited a shift to a larger 2θ after the incorporation of the ZIL, which implies a contraction of the lattice, and this is in stark contrast to the result from the abovementioned reports by Jen et al. and Oh et al.

Pan et al. (2020) reported the use of borohydride (BH₄⁻).^[32] The superhalogen-incorporated perovskite, MAPbI_{3-x}(BH₄)_x, was obtained by using MAPbI₃ precursor solution with the addition of tetrabutylammonium borohydride. The authors suggested that the partial substitution of BH₄⁻ for I⁻ may

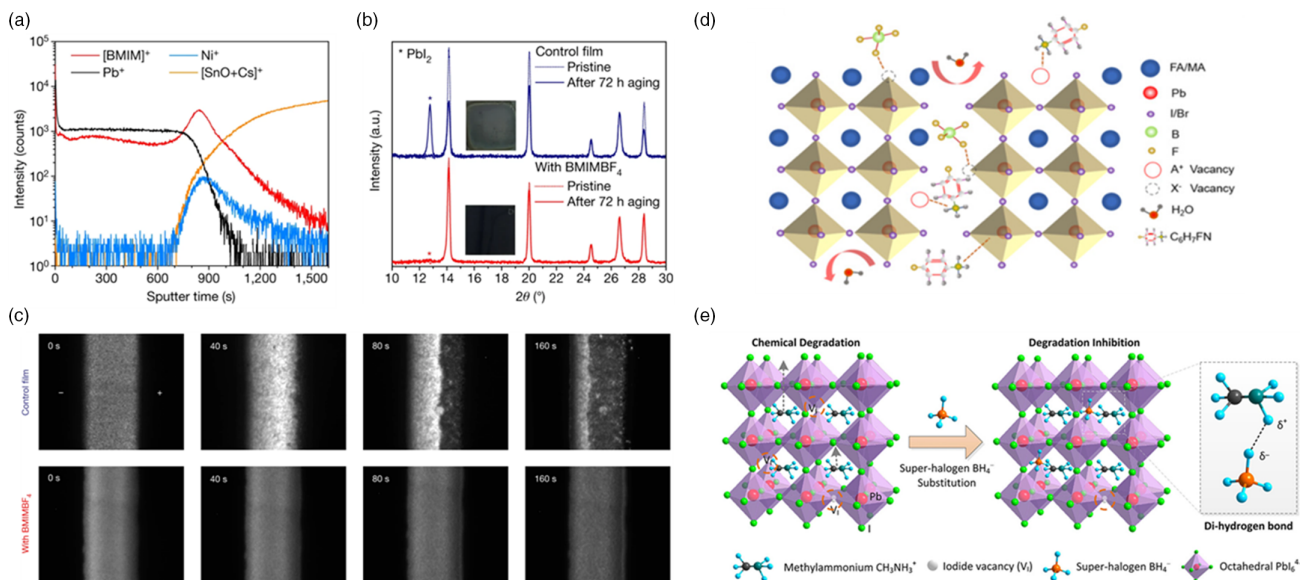


Figure 2. a) Time-of-flight secondary ion mass spectrometry (ToF-SIMS) depth profiles of the 1-butyl-3-methylimidazolium tetrafluoroborate (BMIMBF₄)-containing perovskite film. b) XRD patterns of pristine and aged samples of perovskite films with or without BMIMBF₄. The decomposition of Pbl₂ in the films was denoted as the stars. The inset images show perovskite films after aggressive aging (72 h of light-soaking at 60–65 °C). c) PL images of perovskite films with or without BMIMBF₄ under a constant bias (10 V). Reproduced with permission.^[26] Copyright 2019, Springer Nature. d) Schematic of perovskite lattice that shows defect passivation mechanism by a zwitterionic compound. Reproduced with permission.^[31] Copyright 2021, Wiley-VCH. e) Perovskite lattice before and after the incorporation of superhalogen BH₄⁻, which occupies iodide vacancy and forms hydrogen bonding with MA⁺. Reproduced with permission.^[32] Copyright 2020, American Chemical Society.

compensate V_I so that BH₄⁻ may interact with MA⁺ via dihydrogen bonding (Figure 2e). Therefore, the formation of internal defects and defect migration were effectively suppressed, which led to improvement in the device efficiency and stability. The PSCs using the superhalogen with a structure of FTO/compact-TiO₂/mesoporous-TiO₂/perovskite/spiro-OMeTAD/Au resulted in a PCE of 21.10%, which was higher than that of the control device showing 18.43%. Moreover, current–voltage hysteresis of the PSCs became negligible due to the use of superhalogen.

Although it is generally stated that the use of superhalogen is effective in perovskite defect passivation, there are still unclear and inconsistent points to be clarified, particularly about the incorporation of superhalogen into perovskite lattice. For example, some studies simply surmised that superhalogen occupies the X-site of perovskite lattice by presenting the chemical formula of perovskites as AB(X_γX'_{1-γ})₃ (here, X' denotes superhalogen).^[23,24] Some other works showed a shift in perovskite diffraction peak, which may account for the incorporation of superhalogen into the lattice.^[25,30,31] However, there is a contradiction among these studies regarding whether the perovskite lattice expands or contracts with the superhalogen integrated. On the contrary, another work concluded that superhalogen does not perturbate perovskite lattice as the addition of the compound did not cause a shift of perovskite diffraction peak.^[26] Since there have not been many studies on the use of superhalogen in perovskites, it may be too presumptive to judge whether a claim was erroneous or not. Thus, more clarification to explain these discrepancies seems to be required in follow-up studies.

3. Utilization of Superhalogen for Perovskite Surface Treatment

The surface treatment of perovskites has become widely exploited owing to its notable effects such as reduction of defect density, suppression of nonradiative recombination, protection of underlying perovskite from moisture, and thus improvement in device efficiency and stability. Park et al. (2018) reported the use of FAPF₆ to treat the surface of FA_{0.88}Cs_{0.12}PbI₃ (Figure 3a). The authors suggested that the deposition of FAPF₆ led to partial substitution of PF₆⁻ for iodide by anion exchange which gave rise to the formation of a thin FA_{0.88}Cs_{0.12}PbI_{3-x}(PF₆)_x layer at the surface.^[33] The effect of PF₆⁻ incorporation on crystal structure was investigated by XRD (Figure 3b). Due to the larger ionic radius of PF₆⁻ than I⁻, the first derivative of diffraction peak by (100) exhibited a shift to a lower angle upon an increase in the concentration of PF₆⁻, which implies an increase in lattice constant by replacing I⁻ with PF₆⁻. The superhalogen-incorporated perovskite increased carrier lifetime and decreased defect density, which resulted in the improvement in the photovoltaic performance of PSCs also with reduced current–voltage hysteresis. Moreover, scanning electron microscopy exhibited that the PF₆⁻ integrated perovskite grew preferentially along grain boundaries. Thus, the underlying perovskite layer can be protected from moisture, which improved moisture stability. Chen et al. modulated the surface of perovskite by using phosphonium salts (bromotrisspyrrolidinophosphonium hexafluorophosphate), namely, BrTPPPF₆ containing PF₆⁻.^[34] X-Ray photoelectron spectroscopy (XPS) and density functional theory

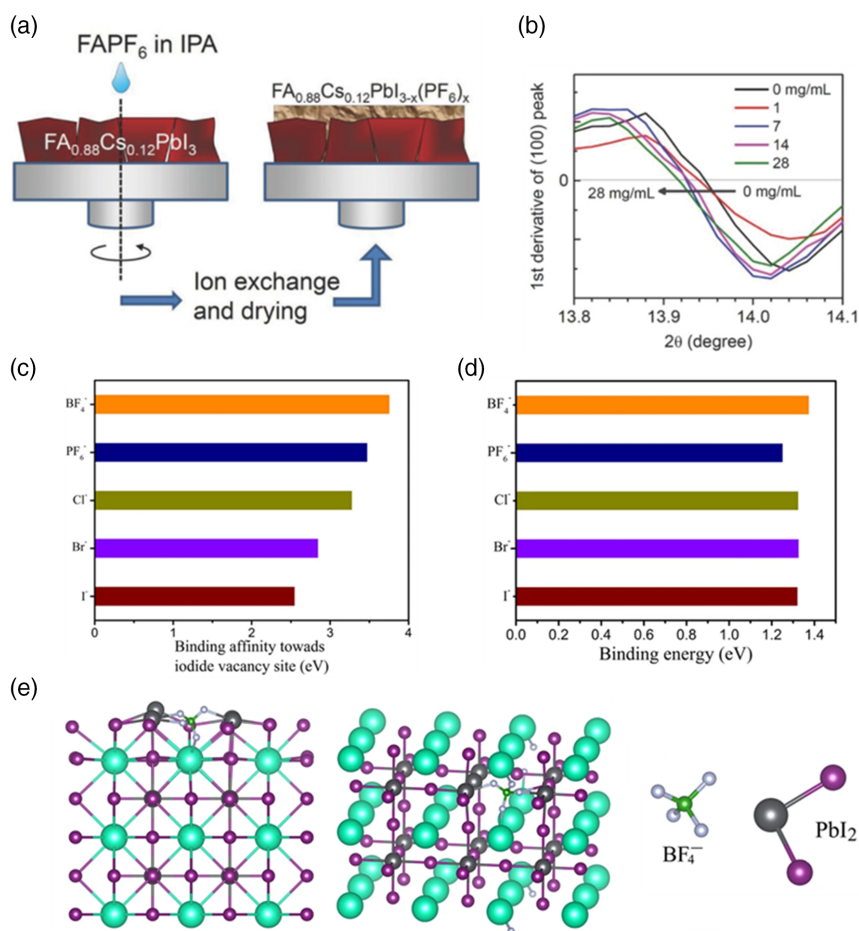


Figure 3. a) Schematic of the formation of superhalogen-incorporated perovskite layer at the surface by anion exchange between I⁻ and PF₆⁻. b) A shift of the first derivative of XRD peak of (100) to low angle as increasing the concentration of FAPF₆. Reproduced with permission.^[33] Copyright 2018, Wiley-VCH. c) The binding affinity of various anions to I⁻ vacancy at the surface of the perovskite (CsPbI₂Br). d) The binding energy of various anions with Pb-I antisite defect. e) Lattice structure showing passivation of an I⁻ vacancy by BF₄⁻ at the surface of perovskite (left) and the interaction between Pb-I antisite and BF₄⁻ (right). Reproduced with permission.^[27] Copyright 2021, Springer Nature.

(DFT) calculations suggested that halide vacancies were filled by PF₆⁻ that passivated undercoordinated Pb²⁺ at the surface of perovskite film. Thus, the surface-treated perovskite had a lower defect density and prolonged carrier lifetimes, which resulted in the PSCs with a PCE of 22.15%, which was higher than the control device (20.6%). Furthermore, as the components of the salt fill the vacancy defects, the authors stated that ion migration and trap-assisted nonradiative recombination were suppressed and moisture resistance improved. Liu et al. (2021) reported the use of imidazolium-based IL containing BF₄ (1-butyl-2,3-dimethylimidazolium tetrafluoroborate) that was applied as a surface passivation agent on top of CsPbI₂Br perovskites.^[27] The authors suggested that BF₄⁻ of the IL played an important role in the passivation of under-coordinated Cs⁺/Pb²⁺ by forming strong ionic interactions (Pb–F, Cs–F). The calculation result corroborated the effectiveness of superhalogen in passivation by showing its higher relative binding affinity than halide to I⁻ vacancy, and also higher binding energy to Pb-I antisite as shown in Figure 3c,d, respectively. In Figure 3e, the passivation of I⁻ vacancy (left) and Pb-I antisite (right) by BF₄⁻ were schematically illustrated.

Nevertheless, since the XRD peak of perovskites did not show an obvious shift with the addition of the IL, the authors concluded that the IL was not incorporated in the perovskite lattice but only passivating the defects at the surface. Thus, PSCs with the surface passivation (FTO/TiO₂/CsPbI₂Br/IL/Spiro-OMeTAD/Au) had a PCE of 17.02% with improved stability whereas the control device exhibited a PCE of 15.62% and rapid degradation. Interestingly, Stranks et al. (2021) suggested a different passivation mechanism by the use of superhalogen.^[35] The authors used MABF₄ for surface treatment of MAPbI₃, and the introduction of BF₄⁻ significantly reduced trap density leading to improvement in PL characteristics with suppressed nonradiative recombination. Importantly, analysis of solid-state nuclear magnetic resonance (NMR) revealed BF₄⁻ did not make an atomic-level interaction with under-coordinated Pb in the perovskite structure. Instead, the reduction of trap density was attributed to BF₄⁻ acting as a scavenger of unreacted methylammonium iodide (MAI) by producing thermodynamically stable MAI–MABF₄ cocrystal, which decreased the concentration of interstitial iodide defects in the perovskite.

The studies introduced in this section would also raise questions primarily about the incorporation of superhalogen in the perovskite lattice and the mechanism of superhalogen passivation. For example, the studies conducted by Park et al. and Chen et al. deduced that superhalogen can occupy the X-site of perovskite lattice by relying on the results of XRD, XPS, and DFT calculations.^[33,34] Thus, the partial substitution of superhalide for the existing halide effectively coordinates the corresponding defective components of perovskites. In contrast, Liu et al. suggested defect passivation by superhalogen only at the surface, but without being incorporated into the perovskite lattice.^[27] In contrast, Stranks et al. strongly corroborated no atomic-scale interaction of superhalogen with the under-coordinated Pb^{2+} in the perovskite lattice by solid-state NMR, which led to their conclusion that superhalogen rather scavenges unreacted MAI.^[35]

4. Conclusion and Outlook

We have presented and discussed studies on the use of superhalogen (e.g., BF_4^- , PF_6^- , and BH_4^-) in perovskites for the

development of efficient and stable PSCs. Highly electronegative superhalogen with a high electron affinity compared to monoatomic halogens may enable the formation of a strong bond to Pb^{2+} and monovalent cations (e.g., MA^+ , FA^+ , and Cs^+) in the bulk or at the surface of perovskites. Accordingly, most of the studies presented in this perspective have addressed that the use of superhalogen was effective in passivation of iodide-related defects (e.g., iodide vacancy and interstitial iodide) in perovskites, showing the reduced density of defects and improved radiative recombination of charge carriers, thereby enhancing efficiency and stability of PSCs. We summarized the improvement of photovoltaic parameters of PSCs after introducing superhalogen into perovskites (**Table 1**).

Nevertheless, there are still unclear aspects of the role of superhalogen in terms of defect passivation. For example, many studies suggested the incorporation of superhalogen into perovskite lattice and chemical or physical interaction between the superhalogen and the perovskite components, which led to defect passivation (e.g., occupation of V_I , interaction with MA^+ via dihydrogen bonding, passivation of undercoordinated Pb^{2+} , Pb-I antisite, lattice strain relaxation, etc.). In contrast, recent work by Stranks et al. revealed that the surface treatment

Table 1. Summary of photovoltaic performance of PSCs before and after introducing superhalogen into PSCs.

Device architecture	Perovskite	Superhalogen compound	V_{oc} [V]	J_{sc} [mA cm^{-2}]	FF	PCE [%]	Remarks	Ref.
Superhalogen in the perovskite bulk								
FTO/(TiO ₂ /ZrO ₂ /carbon)/perovskite	MAPbI ₃	–	0.914	16.92	0.68	10.54		[23]
		MABF ₄	0.957	18.15	0.76	13.24		
FTO/(TiO ₂ /ZrO ₂ /carbon)/perovskite	(5-AVA) _{0.034} MA _{0.966} PbI ₃	–	0.920	22.37	0.65	13.4		[24]
		MABF ₄	0.970	24.37	0.66	15.5		
ITO/SnO ₂ /perovskite/spiro-OMeTAD/MoO ₃ /Ag	(FAPbI ₃) _{0.83} (MAPbBr ₃) _{0.17}	–	1.12	23.39	0.67	17.55		[25]
		NH ₄ BF ₄	1.15	23.38	0.75	20.16		
FTO/NiO/perovskite/PCBM/BCP/Cr/Au	((FA _{0.83} MA _{0.17}) _{0.95} Cs _{0.05} Pb(I _{0.9} Br _{0.1}) ₃)	–	1.02	23.2	0.79	18.5	Under 102 mW cm^{-2}	[26]
		BMIMBF ₄ [–]	1.08	23.8	0.81	19.8	Under 105 mW cm^{-2}	
FTO/polyTPD:F4-TCNQ/perovskite/PCBM/BCP/Cr/Au	Cs _{0.17} FA _{0.83} Pb(I _{1–x} Br _x) ₃	–	1.07	22.4	0.74	17.6		[28]
		[BMP] ⁺ [BF ₄] [–]	1.12	22.7	0.80	20.3		
ITO/PEDOT:PSS/perovskite/PCBM/C ₆₀ /BCP/Ag	FA _{0.5} MA _{0.5} Pb _{0.5} Sn _{0.5} I ₃	–	0.780	30.1	0.735	17.3		[30]
		IMBF ₄	0.810	31.4	0.752	19.1		
ITO/SnO ₂ /perovskite/spiro-OMeTAD/Au	(FAPbI ₃) _{1–x} (MAPbBr ₃) _x	–	1.130	24.00	0.76	20.69		[31]
		[4FB] ⁺ [BF ₄] [–]	1.162	24.85	0.78	22.52		
FTO/c-TiO ₂ /m-TiO ₂ /perovskite/spiro-OMeTAD/Au	MAPbI ₃	–	1.08	21.71	0.781	18.43		[32]
		tetrabutylammonium borohydride	1.11	23.89	0.798	21.10		
Superhalogen at the perovskite surface								
FTO/c-TiO ₂ /m-TiO ₂ /perovskite/spiro-MeOTAD/Au	FA _{0.88} Cs _{0.12} PbI ₃	–	1.020	23.00	0.76	17.79		[33]
		FAPF ₆	1.045	23.11	0.80	19.25		
ITO/SnO ₂ /perovskite/spiro-OMeTAD/Au	(Cs _x Rb _y FA _{1–x–y})Pb(I _{1–a} Br _a) ₃	–	1.133	22.68	0.798	20.61		[34]
		BrTPPPF ₆	1.179	22.95	0.818	22.15		
ITO/TiO ₂ /perovskite/spiro-OMeTAD/Au	CsPbI ₂ Br	–	1.27	15.45	0.779	15.28		[27]
		BMMIMBF ₄	1.31	15.95	0.806	16.89		

of perovskites by superhalogen (BF₄⁻) did not result in its incorporation into the lattice. Instead, a role of the superhalogen compound as a scavenger of unreacted MAI was proposed to decrease the density of interstitial iodide rather than direct passivation of defect sites by superhalogen. The different suggestions might result from various differences, for example, in the target position of the superhalogen treatment, composition of perovskites, deposition process, etc. Thus, further studies are required to verify the bonding state of superhalogen in perovskites and its passivation mechanism. Moreover, unveiling the underlying mechanism of the effective suppression of ion migration by the use of superhalogen may be one of the keys to improvement in the stability of perovskites and PSCs. Given the various types of internal charged defects in perovskites, it may be more practical and effective to exploit zwitterions that contain a functional cationic component as well as superhalide. Thus, the capability of defect passivation may be expanded with a higher degree of freedom in materials selection. We believe that a deeper understanding based on further research on superhalogen in terms of its roles in perovskites may provide a principle and guidelines for the judicious and rational design of superhalogen to improve the efficiency and stability of PSCs.

Acknowledgements

This project has received funding from the European Union's Horizon 2020 research and innovation programme under grant agreement no. 763989 APOLO. This publication was made possible by NPRP grant No. NPRP11S-1231-170150 from the Qatar National Research Fund (a member of the Qatar Foundation).

Open access funding provided by Ecole Polytechnique Federale de Lausanne.

Conflict of Interest

The authors declare no conflict of interest.

Keywords

defect passivation, ion migration, perovskite solar cells, perovskites, superhalogen

Received: January 7, 2022

Revised: March 29, 2022

Published online: April 30, 2022

- [1] A. Kojima, K. Teshima, Y. Shirai, T. Miyasaka, *J. Am. Chem. Soc.* **2009**, *131*, 6050.
- [2] Best Research-Cell Efficiency Chart, <https://www.nrel.gov/pv/cell-efficiency.html>, (accessed: December 2021).
- [3] H. Kim, K.-G. Lim, T.-W. Lee, *Energy Environ. Sci.* **2016**, *9*, 12.
- [4] C. Li, X. Lu, W. Ding, L. Feng, Y. Gao, Z. Guo, *Acta Cryst. B* **2008**, *64*, 702.
- [5] Q. Jiang, Y. Zhao, X. Zhang, X. Yang, Y. Chen, Z. Chu, Q. Ye, X. Li, Z. Yin, J. You, *Nat. Photonics* **2019**, *13*, 460.
- [6] D. Luo, R. Su, W. Zhang, Q. Gong, R. Zhu, *Nat. Rev. Mater.* **2020**, *5*, 44.
- [7] H. Jin, E. Debroye, M. Keshavarz, I. G. Scheblykin, M. B. J. Roeffaers, J. Hofkens, J. A. Steele, *Mater. Horiz.* **2020**, *7*, 397.
- [8] Y. Zhou, I. Poli, D. Meggiolaro, F. De Angelis, A. Petrozza, *Nat. Rev. Mater.* **2021**, *6*, 986.
- [9] B. Chen, P. N. Rudd, S. Yang, Y. Yuan, J. Huang, *Chem. Soc. Rev.* **2019**, *48*, 3842.
- [10] M. V. Kovalenko, L. Protesescu, M. I. Bodnarchuk, *Science* **2017**, *358*, 745.
- [11] A. Mahata, D. Meggiolaro, F. De Angelis, *J. Phys. Chem. Lett.* **2019**, *10*, 1790.
- [12] D. J. Keeble, J. Wiktor, S. K. Pathak, L. J. Phillips, M. Dickmann, K. Durose, H. J. Snaith, W. Egger, *Nat. Commun.* **2021**, *12*, 5566.
- [13] F. Ambrosio, D. Meggiolaro, E. Mosconi, F. D. Angelis, *J. Mater. Chem. A* **2020**, *8*, 6882.
- [14] S. Tan, I. Yavuz, M. H. Weber, T. Huang, C.-H. Chen, R. Wang, H.-C. Wang, J. H. Ko, S. Nuryyeva, J. Xue, Y. Zhao, K.-H. Wei, J.-W. Lee, Y. Yang, *Joule* **2020**, *4*, 2426.
- [15] J. Jeong, M. Kim, J. Seo, H. Lu, P. Ahlawat, A. Mishra, Y. Yang, M. A. Hope, F. T. Eickemeyer, M. Kim, Y. J. Yoon, I. W. Choi, B. P. Darwich, S. J. Choi, Y. Jo, J. H. Lee, B. Walker, S. M. Zakeeruddin, L. Emsley, U. Rothlisberger, A. Hagfeldt, D. S. Kim, M. Grätzel, J. Y. Kim, *Nature* **2021**, *592*, 381.
- [16] H. Lu, Y. Liu, P. Ahlawat, A. Mishra, W. R. Tress, F. T. Eickemeyer, Y. Yang, F. Fu, Z. Wang, C. E. Avalos, B. I. Carlsen, A. Agarwalla, X. Zhang, X. Li, Y. Zhan, S. M. Zakeeruddin, L. Emsley, U. Rothlisberger, L. Zheng, A. Hagfeldt, M. Grätzel, *Science* **2020**, *370*, 6512.
- [17] D. H. Kim, C. P. Muzzillo, J. Tong, A. F. Palmstrom, B. W. Larson, C. Choi, S. P. Harvey, S. Glynn, J. B. Whitaker, F. Zhang, Z. Li, H. Lu, M. F. A. M. van Hest, J. J. Berry, L. M. Mansfield, Y. Huang, Y. Yan, K. Zhu, *Joule* **2019**, *3*, 1734.
- [18] G. L. Gutsev, A. I. Boldyrev, *Russ. Chem. Rev.* **1987**, *56*, 519.
- [19] M. Willis, M. Götz, A. K. Kandalam, G. F. Ganteför, P. Jena, *Angew. Chem. Int. Ed.* **2010**, *49*, 8966.
- [20] S. Nagane, U. Bansode, O. Game, S. Chhatre, S. Ogale, *Chem. Commun.* **2014**, *50*, 9741.
- [21] I. Chung, B. Lee, J. He, R. P. H. Chang, M. G. Kanatzidis, *Nature* **2012**, *485*, 486.
- [22] C. H. Hendon, R. X. Yang, L. A. Burton, A. Walsh, *J. Mater. Chem. A* **2015**, *3*, 9067.
- [23] J. Chen, Y. Rong, A. Mei, Y. Xiong, T. Liu, Y. Sheng, P. Jiang, L. Hong, Y. Guan, X. Zhu, X. Hou, M. Duan, J. Zhao, X. Li, H. Han, *Adv. Energy Mater.* **2016**, *6*, 1502009.
- [24] Y. Sheng, A. Mei, S. Liu, M. Duan, P. Jiang, C. Tian, Y. Xiong, Y. Rong, H. Han, Y. Hu, *J. Mater. Chem. A* **2018**, *6*, 2360.
- [25] J. Zhang, S. Wu, T. Liu, Z. Zhu, A. K.-Y. Jen, *Adv. Funct. Mater.* **2019**, *29*, 1808833.
- [26] S. Bai, P. Da, C. Li, Z. Wang, Z. Yuan, F. Fu, M. Kawecki, X. Liu, N. Sakai, J. T.-W. Wang, S. Huettner, S. Buecheler, M. Fahlman, F. Gao, H. J. Snaith, *Nature* **2019**, *571*, 245.
- [27] J. Xu, J. Cui, S. Yang, Y. Han, X. Guo, Y. Che, D. Xu, C. Duan, W. Zhao, K. Guo, W. Ma, B. Xu, J. Yao, Z. Liu, S. Liu, *Nano-Micro Lett.* **2021**, *14*, 7.
- [28] Y.-H. Lin, N. Sakai, P. Da, J. Wu, H. C. Sansom, A. J. Ramadan, S. Mahesh, J. Liu, R. D. J. Oliver, J. Lim, L. Aspirtate, K. Sharma, P. K. Madhu, A. B. Morales-Vilches, P. K. Nayak, S. Bai, F. Gao, C. R. M. Grovenor, M. B. Johnston, J. G. Labram, J. R. Durrant, J. M. Ball, B. Wenger, B. Stannowski, H. J. Snaith, *Science* **2020**, *369*, 96.
- [29] S. Wang, Y. Jiang, E. J. Juarez-Perez, L. K. Ono, Y. Qi, *Nat. Energy* **2016**, *2*, 1.
- [30] H. Kim, J. W. Lee, G. R. Han, S. K. Kim, J. H. Oh, *Adv. Funct. Mater.* **2021**, *31*, 2008801.

- [31] L. Yang, X. Ma, X. Shang, D. Gao, C. Wang, M. Li, C. Chen, B. Zhang, S. Xu, S. Zheng, H. Song, *Sol. RRL* **2021**, 5, 2100352.
- [32] S. Xu, G. Liu, H. Zheng, X. Xu, L. Zhang, H. Xu, L. Zhu, F. Kong, Y. Li, X. Pan, *ACS Appl. Mater. Interfaces* **2020**, 12, 8249.
- [33] J. Chen, S.-G. Kim, N.-G. Park, *Adv. Mater.* **2018**, 30, 1801948.
- [34] D. He, T. Zhou, B. Liu, L. Bai, W. Wang, H. Yuan, C. Xu, Q. Song, D. Lee, Z. Zang, L. Ding, J. Chen, *EcoMat* **2022**, 4, 12158.
- [35] S. Nagane, S. Macpherson, M. A. Hope, D. J. Kubicki, W. Li, S. D. Verma, J. Ferrer Orri, Y.-H. Chiang, J. L. MacManus-Driscoll, C. P. Grey, S. D. Stranks, *Adv. Mater.* **2021**, 33, 2102462.